HHS Public Access

Author manuscript

Inorg Chem. Author manuscript; available in PMC 2023 October 30.

Published in final edited form as:

Inorg Chem. 2020 February 03; 59(3): 2083–2091. doi:10.1021/acs.inorgchem.9b03572.

Coordination-Assisted Reversible Photoswitching of Spiropyran-Based Platinum Macrocycles

Soumalya Bhattacharyya[‡],
Department of Inorganic and Physical Chemistry, Indian Institute of Science, Bangalore 560012, India

Manoranjan Maity[‡],
Department of Inorganic and Physical Chemistry, Indian Institute of Science, Bangalore 560012, India

Aniket Chowdhury,
Department of Inorganic and Physical Chemistry, Indian Institute of Science, Bangalore 560012, India; Department of Industrial Chemistry, Mizoram University, Aizawl 796004, India

Manik Lal Saha,
Department of Chemistry, University of Utah, Salt Lake City, Utah 84112, United States

Sumit Kumar Panja,
Department of Inorganic and Physical Chemistry, Indian Institute of Science, Bangalore 560012, India

Peter J. Stang,
Department of Chemistry, University of Utah, Salt Lake City, Utah 84112, United States

Partha Sarathi Mukherjee
Department of Inorganic and Physical Chemistry, Indian Institute of Science, Bangalore 560012, India

Abstract

Control over the stimuli-responsive behavior of smart molecular systems can influence their capability to execute complex functionalities. Herein, we report the development of a suite of spiropyran-based multi-stimuli-responsive self-assembled platinum(II) macrocycles (**5**–**7**), rendering coordination-assisted enhanced photochromism relative to the corresponding ligands. **5** showed shrinking and swelling during photoreversal, while **6** and **7** are fast and fatigue-free supramolecular photoswitches. **6** turns out to be a better fatigue-resistant photoswitch and can

Corresponding Authors stang@chem.utah.edu; psm@iisc.ac.in.

[‡]Author Contributions
These authors have contributed equally.

Supporting Information
The Supporting Information is available free of charge at https://pubs.acs.org/doi/10.1021/acs.inorgchem.9b03572.
Experimental procedures, multinuclear NMR (^{1}H, ^{31}P, ^{13}C, DOSY, and COSY), MS, and UV–vis spectra, and the DFT and TD-DFT results (PDF)

Complete contact information is available at: https://pubs.acs.org/10.1021/acs.inorgchem.9b03572

The authors declare no competing financial interest.

retain an intact photoswitching ability of up to 20 reversible cycles. The switching behavior of the macrocycles can also be precisely controlled by tuning the pH of the medium. Our present strategy for the construction of rapid stimuli-responsive supramolecular architectures via coordination-driven self-assembly represents an efficient route for the development of smart molecular switches.

Graphical Abstract

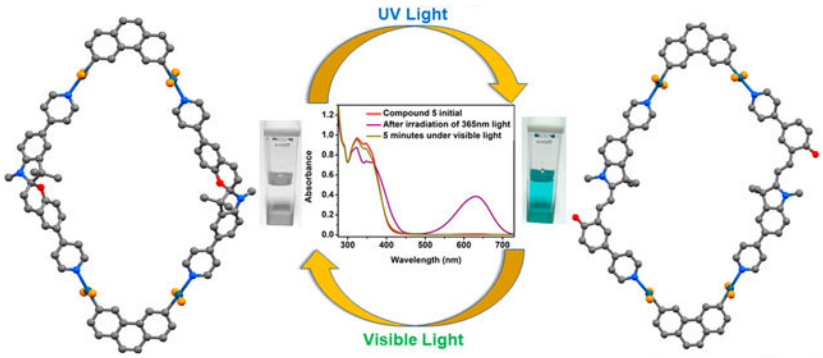

INTRODUCTION

Nature has a wide range of species (cephalopods, chameleons, insects, and bacteria) that reversibly change their color or structure in response to various environmental stimuli.[1] These living organisms in response to a sudden change in their environment, such as light, heat, or shock, use complex mechanisms involving self-assembled biosupramolecules to accomplish the desired change in their body coloration. When such stimuli-responsive behavior is mimicked in artificial systems, sophisticated architectures with tunable functionality can be achieved.[2] A wide array of external stimuli including pH,[3] electrochemical potential,[4] magnetic field,[5] light,[6] mechanical shock, and sound wave may be used to induce structural changes in smart molecules. Among them, light is of particular importance because it functions rapidly,[7] and the transformations induced by light generally do not produce byproducts even after multiple cycles.[8]

In a molecular system, the photoresponsive units can be incorporated using various methodologies including covalent attachment, supramolecular interaction, and host–guest chemistry. The covalent attachment approach to design molecular architectures with multiple numbers of photochromic units has several disadvantages: multistep synthesis, a tedious purification process, low final yield, etc. Supramolecular self-assembly using noncovalent metal–ligand bond formation is a great alternative tool to achieve discrete systems decorated with multiple functional moieties.[9] Specific numbers of desired photoactive functional groups can be appended in supramolecular coordination architectures by simply attaching suitable functional groups either to the metal acceptors or to the organic donors.[10] These architectures have several positive attributes, including simple synthesis, high yield, and kinetic reversibility, that provide the chance of self-repairing the final product.[11]

Photoinduced reversible transformation of coordination architectures has fascinated researchers because of its precise control over structural isomers during photoirradiation.[12] Most of these architectures have extensively used diarylethenes or azobenzenes as the photoactive unit.[13] Nevertheless, they have been marred with several shortcomings including slow reversibility and structural fatigue, and oftentimes the change in the signal is not large enough because of the similarity of the two structural forms. Structures derived using other photochromic units, such as chromene, stilbene, and a donor–acceptor Stenhouse adduct,[14] have also been characterized with the aforementioned drawbacks and exhibit poor solubility in common solvents, making their synthesis difficult. In contrast, spiropyran is an excellent photochromic unit and has found many applications in data storage,[15] smart materials,[16] sensors,[17] light-harvesting units,[18] and biological imaging,[19] because of its vast difference in color and absorption profiles between the ring-opened and -closed forms[20] as well as its high solubility and drastic change in polarity. Hence, supramolecular photoswitches comprising a spiropyran unit could be of importance in circumventing the aforesaid issues. Most of the spiropyran-based discrete molecular systems have a spiropyran unit in the periphery of the architecture, and they suffer from very fast photoisomerization, leading to a small lifetime of the ring-opened state.[21] It is proposed that if the spyropyran moiety is incorporated directly into the backbone of the architecture, upon photoirradiation, not only can the structural change of the whole architecture be achieved but also the time taken for photoisomerization can be precisely controlled. Thus, photoirradiation will lead to a breathing supramolecular photoswitch.

Herein, we describe the synthesis of spiropyran-functionalized dipyridyl donors (**1** and **2**) and their use in the construction of supramolecular photoswitches (**5**–**7**), which show metal-coordination-assisted enhanced photochromism (Scheme 1). **6** is a durable, fatigue-free, fast photoswitch where photochromism occurs at the peripheral position, whereas the photochromic macrocycle **5** exhibits shrinking and swelling during photoreversal because of the presence of spiropyran in the backbone. To the best of our knowledge, **5** represents the first example of a discrete supramolecular architecture in which spiropyran is present in the backbone. All of the macrocycles show acidochromism because of the protonation–deprotonation equilibrium of the spiropyran unit.

RESULTS AND DISCUSSION

Synthesis and Characterization.

The spiropyran-functionalized dipyridyl building block **1** was synthesized by a palladium-catalyzed Suzuki cross-coupling reaction between dibromospiropyran[22] (**A**) and 4-pyridinylboronic acid (Scheme S1). The other spiropyran-based 120° donor **2** was synthesized following the conventional Sonogashira coupling reaction of *N*,*N*-bis(4-pyridyl)-4-iodoaniline (**C**) with freshly prepared alkyne-functionalized spiropyran (Scheme S2).[23] Donors **1** and **2** were fully characterized by multinuclear NMR and electrospray ionization mass spectrometry (ESI-MS) analyses (Figures S1-S6).

Donor **1** was reacted with a 60° organoplatinum(II) acceptor, 2,9-bis[*trans*-$Pt(PEt_3)_2NO_3$]phenanthrene (**3**), in dry dichloromethane at 40 °C for 12 h, and then

the solvent was concentrated to a minimum amount, which, upon treatment with cold diethyl ether, afforded pure macrocycle **5** as a precipitate. Donor **2** was separately treated with **3** in similar manner and with cis-protected (tmen)Pt(NO_3)$_2$ (**4;** tmen = *N*,*N*,*N*′,*N*′-tetramethylethane-1,2-diamine) in an acetone/methanol (1:1) mixture at 50 °C for 12 h, which resulted in the formation of macrocycles **6** and **7**, respectively (Schemes 2 and S4-S6). The formation of a single macrocycle in both cases was confirmed by multinuclear NMR (^{1}H, ^{31}P, and ^{13}C) and 2D diffusion-ordered ^{1}H (DOSY) NMR analyses.

In the ^{1}H NMR spectrum of the macrocycle **6,** one of the α-pyridine protons (H_a) exhibited a downfield shift ($\Delta\delta$ = 0.39 ppm) and the other one was upfield-shifted ($\Delta\delta$ = 0.15 ppm) compared to the free ligand (**2**; Figure 1). These downfield and upfield shifts were observed because of the difference in the electron density generated at the *a*/*a*′ and *b*/*b*′ positions upon coordination of the pyridine N atom to the Pt(II) metal center. Meanwhile, the singlet peak at 8.48 ppm and the other three peaks at 7.58–7.41 ppm of a 60° platinum acceptor (Figure S7) on the phenanthrene ring were downfield-shifted to a singlet at 8.66 ppm and a multiplet at 7.58–7.53 ppm, respectively. A significant downfield shift of other protons of **2** was observed because of metal–ligand complexation. A quite similar downfield shift in the α-pyridyl protons was observed for macrocycle **7** as well.

The ^{31}P NMR spectrum supported the formation of one product because only a single peak was observed for both the macrocycles **5** and **6**. For **6,** a peak at 13.83 ppm is significantly upfield-shifted in comparison with the 60° platinum acceptor **3** (18.50 ppm). This change, as well as a decrease in the coupling of the flanking ^{195}Pt satellites [ΔJ(Pt,P) ≈ −265 Hz], was consistent with electron back-donation from the Pt(II) ion. The macrocycle **5** also showed a similar upfield shift from 18.50 to 12.93 ppm with ΔJ(Pt,P) ≈−290 Hz (Figure 2). Single vertical traces in the 2D ^{1}H DOSY NMR spectra for all of the three macrocycles also confirmed the formation of a single product in these complexation reactions (Figures S11, S14, and S16).

Metal ligand coordination was clearly evident from the multinuclear NMR analysis, but it could not indicate the composition of the macrocycles. The stoichiometry of the building blocks and the formation of bis(spirospyran)-functionalized macrocycles (**5**–**7**) were established by ESI-MS analysis.

In the MS spectrum of **5,** peaks corresponding to the [**5** – 2NO_3]$^{2+}$ (*m*/*z* 1531.8307), [**5** – 3NO_3]$^{3+}$(*m*/*z* 1000.9058), and [**5** – 4NO_3]$^{4+}$ (*m*/*z* 734.9351) fragments were observed. For **6,** the signal for the [**6** – 3NO_3]$^{3+}$ (*m*/*z* 1077.78) fragment along with [**6** – 2NO_3]$^{2+}$ (*m*/*z* 1647.68) was found in the spectrum. The isotopic patterns of these peaks were well resolved and matched properly with the simulated patterns (Figures 3 and S17-S22). Similarly, for 7, the *m*/*z* 592.57 and 1901.64 peaks corresponding to the [7 – 3NO_3]$^{3+}$ and [7 – NO_3]$^{+}$ fragments, respectively, were present in the MS spectrum and were in good agreement with the calculated values (Figures S21 and S22). All of these signals and their well-resolved isotopic patterns support the formation of [2 + 2] macrocycles.

Single crystals suitable for X-ray diffraction could not be obtained after many attempts. To gain further insight into the structures of the macrocycles and building blocks, their

geometries were optimized using the PM6 method, where ethyl groups of the phosphine ligands were modeled as H atoms. **1** has a bite angle of ~134° in the close form which reduces to ~125° in the open form. A bite angle closer to 120° supports formation of the [2 + 2] macrocyle (**5**). Compound **5** has an oval-shaped structure with a coplanar geometry. **6** is found to be planar with a rhomboid shape, whereas 7 has a bent structure due to the presence of the 90° platinum(II) building block (Figure 4).

Photochromism.

The photoisomerization behavior was investigated using 365 nm irradiation with dimethyl sulfoxide (DMSO) as the solvent. When the spiropyran transforms to its ring-opened form upon light irradiation, it becomes more polar in comparison to its ring-closed form because of the generation of charge-separated species (Scheme 3). The use of a polar solvent like DMSO can not only stabilize the more polar open structure but also increase the solubility of the complex.

The photochromism was monitored by UV–vis spectroscopy. When donor **1** was exposed to light irradiation (365 and 254 nm), no color change was observed even after 15 min of exposure. Donor **2** also showed similar results (Figures S29 and S30). In contrast, the DMSO solution of **5** gave an intense blue coloration from an almost colorless solution upon irradiation for 2 min with 365 nm light. The absorbance of the band at 347 nm decreased, and a new peak was observed at 632 nm. This is attributed to the formation of an open merocyanine structure of spiropyran, which was facilitated by metal–ligand coordination. The blue solution returned to its initial state within 5 min of exposure to visible light. The peak at 632 nm vanished, and the absorption profile was like that of the initial (Figure 5a) form. In the case of **6,** the absorption maximum at 328 nm was lowered, and the peak corresponding to the open form appeared at 623 nm with intense-blue coloration. The reversibility was very fast in this case; within 2 min, the blue merocyanine form changed to its initial ring-closed colorless spiropyran form (Figure 5b). Very similar photochromic behavior was observed for 7 as well, where the color change was observed in 2 min and at 621 nm an intense band appeared in the UV–vis spectrum (Figure S31a).

Upon examination of the optimized structure, **5** showed shrinkage upon going from a closed form to an open form after light irradiation, and the distance between the two spiro C atoms of the opposite spiropyrans was found to decrease by 1 Å (Figure S23). This is due to the structural change of the spiropyran backbone of **1** in **5** during photoisomerization. For **5,** we observed that the open form stays for 5 min, which is greater in comparison to **6** and **7**. This can be attributed to the fact that the bite angle of donor **1** changes from 134° to 125° after ring opening (Figure 4). Thus, it may be assumed that more electron density can be transferred through coordination to a metal ion as the angle gets closer to 120°, making the open form more stable.

Because the macrocycles showed fast reversible photoisomerization, it was important to verify the extent of the photoswitching ability because for practical applications it is crucial to have good photoreversibility. Thus, DMSO solutions of these macrocycles were repeatedly exposed to UV and visible light, and their absorption spectra were recorded.

6 showed excellent photostability over a period of 20 cycles, with a negligible amount of lowering of the absorption intensity for the open form, whereas **5** started to degrade after 5 cycles (Figure 6). This is due to the positional difference of the spiropyran in the macrocycles. For **6,** the spiropyran unit is in the periphery, and so during photoisomerization it does not disturb the geometry of the macrocycle, which avoids any sort of photofatigue. In contrast, the spiropyran unit is present in the backbone in **5,** and hence the macrocycle swells and shrinks during photoisomerization, which may rupture the self-assembly after a few cycles because of variable bite angles of the closed and open forms of donor **1**. **7** was found to be a good reversible photoswitch for up to 10 cycles (Figure S31b).

Because of the short lifetime of the open forms, attempts to obtain NMR data were unsuccessful. Time-dependent density functional theory (TD-DFT) was performed to get a better understanding of the photochromism. For **5,** the UV–vis band for the open form was found to be very close to the experimental results, suggesting that a well-controlled photoinduced transformation has been successfully achieved (Figure 7). Because the open merocyanine form is more polar as a result of charge separation, any group that can draw electron density toward itself from the spiro ring would favor photoisomerization. In the case of both donors (**1** and **2**), aryl moieties are attached to the spiro ring, which increases the electron density over the spiro ring and restricts photochromism. However, when it coordinates to the Pt(II) metal ions, the electron density gets transferred to the acceptor from the pyridyl rings, which is evident from the downfield shift of the pyridyl protons in ^{1}H NMR. Thus, it escalates the ring opening, and photochromism occurs at ambient conditions upon coordination. This was also shown via electron density mapping in our previous report.[24] The Pt(II) metal ion being a heavy atom can act as an intramolecular photosensitizer which also may accelerate the photoswitching.[25] N-methylation of donor **2** was performed (Scheme S7) to partially reduce the electron density over the spiropyran, and its photochromism was studied (Figure S34). We did not observe any photochromism of the N-methylated pyridinium salt (**8**) at ambient conditions, which also strengthens the hypothesis of metal-ion-coordination-assisted photochromism.

The structural isomers (open form) of the photochromic macrocycles were easily converted to their original conformations (closed form) in the absence of light. To arrest the ring-opened merocyanine (MC) forms, dilute (2 N) HNO_3 (a DMSO solution) was added to the DMSO solutions of the macrocycles. No change was observed in room light, but after irradiation with 365 nm UV light for 2 min, the colorless solutions became intense yellow. As soon as the spiro ring opened, the negatively charged O captured the proton from the medium and formed a protonated merocyanine (MCH^+) with yellow coloration. When the proton was removed by the addition of a dilute solution of base (triethylamine), the yellow solution turned blue (MC form), and upon subsequent exposure to visible light, the initial spiro (SP) form of the molecule was regenerated (Scheme S8). This acid chromism was confirmed by a UV–vis study, which showed a new band at 447 nm for **6** upon irradiation of 365 nm light for 2 min in the presence of dilute acid. When an equivalent amount of base was added to the medium, the band for the MC form at 625 nm (**6**) regenerated and then vanished upon further exposure to visible light (Figure 8). In a similar way, new bands at 452 and 449 nm were observed for the MCH^+ form for **5** and **7,** respectively (Figures S35

and S36). The time to go back to the initial colorless form is 3 times more for **5** compared to that for **6** and **7**. This also stems from the positional difference of spiropyran in the macrocycles. Because the open protonated form is stable enough, we tried to explore the ^{1}H NMR of the merocyanine form as well. Upon treatment with dilute HNO_3 and UV light (365 nm), significant displacement of the proton peaks was observed and was reversibly restored when neutralized with a base (Figure S37 and S38. Thus, these platinum(II) macrocycles are not only photoresponsive but also acidochromic.

CONCLUSION

In conclusion, two spiropyran-based dipyridyl ligands (**1** and **2**) were employed to construct three [2 + 2] self-assembled platinum(II) macrocycles (**5**–**7**) in an efficient manner via the directional coordination self-assembly approach. In **1,** the spiropyran unit is in the backbone, whereas in **2,** the spiropyran resides on the periphery, which dictated the nature of the photochromism in the final macrocycles. Essentially nonphotochromic ligands gave rise to fast and reversible phtochromic macrocycles upon metal–ligand coordination. **5** is the first example of a discrete coordination architecture as a photoswitch where spiropyran resides in the backbone of the architecture, and it showed photoinduced structural changes during photoreversal, having efficient photoswitching ability for up to 5 cycles. On the other hand, **6** is an excellent fatigue-free supramolecular photoswitch showing efficient reversibility for up to 20 reversible cycles. 7 also showed comparable photochromic behavior, which reconfirms the idea of coordination-driven enhanced photochromism. This work fulfills the requirement of fast supramolecular photoswitches and could pave the way for the development of new smart materials.

Supplementary Material

Refer to Web version on PubMed Central for supplementary material.

ACKNOWLEDGMENTS

P.S.M. and S.B. thank the CSIR (New Delhi, India) for financial support. M.M. and S.K.P. are grateful to Dr. D. S. Kothari and for a national postdoctoral fellowship, respectively.

REFERENCES

(1). Stuart-Fox D; Moussalli A Camouflage, communication and thermoregulation: lessons from colour changing organisms. Philos. Trans. R. Soc., B 2009, 364, 463.

(2)(a). Dublin SN; Conticello VP Design of a Selective Metal Ion Switch for Self-Assembly of Peptide-Based Fibrils. J. Am. Chem. Soc 2008, 130, 49. [PubMed: 18067302] (b)Kudernac T; Ruangsupapichat N; Parschau M; Maciá B; Katsonis N; Harutyunyan SR; Ernst K-H; Feringa BL Electrically driven directional motion of a four-wheeled molecule on a metal surface. Nature 2011, 479, 208. [PubMed: 22071765] (c)Yan X; Wang F; Zheng B; Huang F Stimuli-responsive supramolecular polymeric materials. Chem. Soc. Rev 2012, 41, 6042. [PubMed: 22618080] (d)Chen L-J; Yang H-B Construction of Stimuli-Responsive Functional Materials via Hierarchical Self-Assembly Involving Coordination Interactions. Acc. Chem. Res 2018, 51, 2699. [PubMed: 30285407]

(3)(a). Grunder S; McGrier PL; Whalley AC; Boyle MM; Stern C; Stoddart JF A Water-Soluble pH-Triggered Molecular Switch. J. Am. Chem. Soc 2013, 135, 17691. [PubMed: 24199630] (b)Li Y; Zhao T; Wang C; Lin Z; Huang G; Sumer BD; Gao J Molecular basis of cooperativity in

pH-triggered supramolecular self-assembly. Nat. Commun 2016, 7, 13214. [PubMed: 27786266] (c)Lim E-K; Huh Y-M; Yang J; Lee K; Suh J-S; Haam S pH-Triggered Drug-Releasing Magnetic Nanoparticles for Cancer Therapy Guided by Molecular Imaging by MRI. Adv. Mater 2011, 23, 2436. [PubMed: 21491515]

(4)(a). Adhikari B; Kraatz H-B Redox-triggered changes in the self-assembly of a ferrocene-peptide conjugate. Chem. Commun 2014, 50, 5551.(b)Benyettou F; Zheng X; Elacqua E; Wang Y; Dalvand P; Asfari Z; Olsen J-C; Han DS; Saleh N. i.; Elhabiri M; Weck M; Trabolsi A Redox-Responsive Viologen-Mediated Self-Assembly of CB[7]-Modified Patchy Particles. Langmuir 2016, 32, 7144. [PubMed: 27323835] (c)Bucher C; Moutet J-C; Pécaut J; Royal G; Saint-Aman E; Thomas F Redox-Triggered Molecular Movement in a Multicomponent Metal Complex in Solution and in the Solid State. Inorg. Chem 2004, 43, 3777. [PubMed: 15206851] (d)Yang H-S; Jang J; Lee B-S; Kang T-H; Park J-J; Yu W-R Redox-Triggered Coloration Mechanism of Electrically Tunable Colloidal Photonic Crystals. Langmuir 2017, 33, 9057. [PubMed: 28806515]

(5)(a). Sahoo Y; Cheon M; Wang S; Luo H; Furlani EP; Prasad PN Field-Directed Self-Assembly of Magnetic Nanoparticles. J. Phys. Chem. B 2004, 108, 3380.(b)Zakharchenko A; Guz N; Laradji AM; Katz E; Minko S Magnetic field remotely controlled selective biocatalysis. Nat. Catal 2018, 1, 73.

(6)(a). Gilat SL; Kawai SH; Lehn J-M Light-Triggered Molecular Devices: Photochemical Switching Of optical and Electrochemical Properties in Molecular Wire Type Diarylethene Species. Chem. - Eur. J 1995, 1, 275.(b)Lubbe AS; Liu Q; Smith SJ; de Vries JW; Kistemaker JCM; de Vries AH; Faustino I; Meng Z; Szymanski W; Herrmann A; Feringa BL Photoswitching of DNA Hybridization Using a Molecular Motor. J. Am. Chem. Soc. 2018, 140, 5069. [PubMed: 29551069] (c)Neilson BM; Bielawski CW Photoswitchable Organocatalysis: Using Light To Modulate the Catalytic Activities of N-Heterocyclic Carbenes. J. Am. Chem. Soc. 2012, 134, 12693. [PubMed: 22809240] (d)Szewczyk M; Sobczak G; Sashuk V Photoswitchable Catalysis by a Small Swinging Molecule Confined on the Surface of a Colloidal Particle. ACS Catal. 2018, 8, 2810.

(7)(a). Chen S; Chen L-J; Yang H-B; Tian H; Zhu W Light-Triggered Reversible Supramolecular Transformations of Multi-Bisthienylethene Hexagons. J. Am. Chem. Soc 2012, 134, 13596. [PubMed: 22881042] (b)Han M; Michel R; He B; Chen Y-S; Stalke D; John M; Clever GH Light-Triggered Guest Uptake and Release by a Photochromic Coordination Cage. Angew. Chem., Int. Ed 2013, 52, 1319.(c)Samanta D; Mukherjee PS Sunlight-Induced Covalent Marriage of Two Triply Interlocked Pd6 Cages and Their Facile Thermal Separation. J. Am. Chem., Soc 2014, 136, 17006. [PubMed: 25423470] (d)Sun S-S; Anspach JA; Lees AJ Self-Assembly of Transition-Metal-Based Macrocycles Linked by Photoisomerizable Ligands: Examples of Photoinduced Conversion of Tetranuclear-Dinuclear Squares. Inorg. Chem 2002, 41, 1862. [PubMed: 11925181]

(8). Göstl R; Senf A; Hecht S Remote-controlling chemical reactions by light: Towards chemistry with high spatio-temporal resolution. Chem. Soc. Rev 2014, 43, 1982. [PubMed: 24413363]

(9) (a). Bunzen J; Bruhn T; Bringmann G; Lützen A Synthesis and helicate formation of a new family of BINOL-based bis (bipyridine) ligands. J. Am. Chem. Soc 2009, 131, 3621. [PubMed: 19231865] (b)Bunzen J; Hovorka R; Lützen A Surprising Substituent Effects on the Self-Assembly of Helicates from Bis (bipyridyl) BINOL Ligands. J. Org. Chem 2009, 74, 5228. [PubMed: 19518073] (c)Hardy M; Struch N; Topić F; Schnakenburg G; Rissanen K; Lützen A Stepwise Construction of Heterobimetallic Cages by an Extended Molecular Library Approach. Inorg. Chem 2018, 57, 3507. [PubMed: 29185725] (d)Li Y; Jiang Z; Wang M; Yuan J; Liu D; Yang X; Chen M; Yan J; Li X; Wang P Giant, Hollow 2D metalloarchitecture: Stepwise self-assembly of a hexagonal supramolecular nut. J. Am. Chem. Soc 2016, 138, 10041. [PubMed: 27447878] (e)Sun Y; Li S; Zhou Z; Saha ML; Datta S; Zhang M; Yan X; Tian D; Wang H; Wang L; Li X; Liu M; Li H; Stang PJ Alanine-Based Chiral Metallogels via Supramolecular Coordination Complex Platforms: Metallogelation Induced Chirality Transfer. J. Am. Chem. Soc 2018, 140, 3257. [PubMed: 29290113] (f)Yan X; Cook TR; Pollock JB; Wei P; Zhang Y; Yu Y; Huang F; Stang PJ Responsive Supramolecular Polymer Metallogel Constructed by Orthogonal Coordination-Driven Self-Assembly and Host/Guest Interactions. J. Am. Chem. Soc 2014, 136, 4460. [PubMed: 24621148] (g)Yan X; Jiang B; Cook TR; Zhang Y; Li J; Yu Y; Huang F;

Yang H-B; Stang PJ Dendronized organoplatinum (II) metallacyclic polymers constructed by hierarchical coordination-driven self-assembly and hydrogen-bonding interfaces. J. Am. Chem. Soc 2013, 135, 16813. [PubMed: 24187961] (h)Yu G; Zhang M; Saha ML; Mao Z; Chen J; Yao Y; Zhou Z; Liu Y; Gao C; Huang F; Chen X; Stang PJ Antitumor activity of a unique polymer that incorporates a fluorescent self-assembled metallacycle. J. Am. Chem. Soc 2017, 139, 15940. [PubMed: 29019660] (i)Yu G; Zhao X; Zhou J; Mao Z; Huang X; Wang Z; Hua B; Liu Y; Zhang F; He Z; Jacobson O; Gao C; Wang W; Yu C; Zhu X; Huang F; Chen X Supramolecular Polymer-Based Nanomedicine: High Therapeutic Performance and Negligible Long-Term Immunotoxicity. J. Am. Chem. Soc 2018, 140, 8005. [PubMed: 29874067]

(10) (a). Hauke CE; Oldacre AN; Fulong CRP; Friedman AE ; Cook TR Coordination-Driven Self-Assembly of Ruthenium Polypyridyl Nodes Resulting in Emergent Photophysical and Electrochemical Properties. Inorg. Chem 2018, 57, 3587. [PubMed: 29278500] (b)Hong CM; Kaphan DM; Bergman RG; Raymond KN; Toste FD Conformational Selection as the Mechanism of Guest Binding in a Flexible Supramolecular Host. J. Am. Chem. Soc 2017, 139, 8013. [PubMed: 28581740] (c)Johnson DW; Raymond KN The Self-Assembly of a [Ga4 L 6] 12-Tetrahedral Cluster Thermodynamically Driven by Host- Guest Interactions. Inorg. Chem 2001, 40, 5157. [PubMed: 11559075] (d)Luis ET; Iranmanesh H; Arachchige KS; Donald WA; Quach G; Moore EG; Beves JE Luminescent Tetrahedral Molecular Cages Containing Ruthenium (II) Chromophores. Inorg. Chem 2018, 57, 8476. [PubMed: 29969245] (e)Preston D; Lewis JE; Crowley JD Multicavity [Pd n L4] 2 n+ Cages with Controlled Segregated Binding of Different Guests. J. Am. Chem. Soc 2017, 139, 2379. [PubMed: 28110525] (f)Saha ML; Yan X; Stang PJ Photophysical properties of organoplatinum (II) compounds and derived self-assembled metallacycles and metallacages: Fluorescence and its applications. Acc. Chem. Res 2016, 49, 2527. [PubMed: 27736060] (g)Wu N-W; Zhang J; Ciren D; Han Q; Chen L-J; Xu L; Yang H-B Construction of Supramolecular Pyrene-Modified Metallacycles via Coordination-Driven Self-Assembly and Their Spectroscopic Behavior. Organometallics 2013, 32, 2536.(h)Elliott ABS; Lewis JEM; van der Salm H; McAdam CJ; Crowley JD; Gordon KC Luminescent Cages: Pendant Emissive Units on [Pd2L4]4+ “Click” Cages. Inorg. Chem 2016, 55, 3440. [PubMed: 26991000] (i)Sepehrpour H; Fu W; Sun Y; Stang PJ Biomedically Relevant Self-Assembled Metallacycles and Metallacages. J. Am. Chem. Soc 2019, 141, 14005. [PubMed: 31419112] (j)Acharyya K; Bhattacharyya S; Sepehrpour H; Chakraborty S; Lu S; Shi B; Li X; Mukherjee PS; Stang PJ Self-Assembled Fluorescent Pt(II) Metallacycles as Artificial Light-Harvesting Systems. J. Am. Chem. Soc 2019, 141, 14565. [PubMed: 31479260] (k)Jiang B; Zhang J; Ma J-Q; Zheng W; Chen L-J; Sun B; Li C; Hu B-W; Tan H; Li X; Yang H-B Vapochromic Behavior of a Chair-Shaped Supramolecular Metallacycle with Ultra-Stability. J. Am. Chem. Soc 2016, 138, 738. [PubMed: 26741405] (l)Chen L-J; Ren Y-Y; Wu N-W; Sun B; Ma J-Q; Zhang L; Tan H; Liu M; Li X; Yang H-B Hierarchical Self-Assembly of Discrete Organoplatinum(II) Metallacycles with Polysaccharide via Electrostatic Interactions and Their Application for Heparin Detection. J. Am. Chem. Soc 2015, 137, 11725. [PubMed: 26322626]

(11) (a). Cheng K-Y; Wang S-C; Chen Y-S; Chan Y-T Self-Assembly and Catalytic Reactivity of BINOL-Bridged Bis-(phenanthroline) Metallocages. Inorg. Chem 2018, 57, 3559. [PubMed: 29140082] (b)Holloway LR; Bogie PM; Lyon Y; Ngai C; Miller TF; Julian RR; Hooley RJ Tandem Reactivity of a Self-Assembled Cage Catalyst with Endohedral Acid Groups. J. Am. Chem. Soc 2018, 140, 8078. [PubMed: 29913069] (c)Howlader P; Das P; Zangrando E; Mukherjee PS Urea-Functionalized Self-Assembled Molecular Prism for Heterogeneous Catalysis in Water. J. Am. Chem. Soc 2016, 138, 1668. [PubMed: 26771202] (d)Inokuma Y; Kawano M; Fujita M Crystalline molecular flasks. Nat. Chem 2011, 3, 349. [PubMed: 21505492] (e)Kaphan DM; Toste FD; Bergman RG; Raymond KN Enabling New Modes of Reactivity via Constrictive Binding in a Supramolecular-Assembly-Catalyzed Aza-Prins Cyclization. J. Am. Chem. Soc 2015, 137, 9202. [PubMed: 26176416] (f)Kawamichi T; Haneda T; Kawano M; Fujita M X-ray observation of a transient hemiaminal trapped in a porous network. Nature 2009, 461, 633. [PubMed: 19794489] (g)Martí-Centelles V; Lawrence AL; Lusby PJ High Activity and Efficient Turnover by a Simple, Self-Assembled “Artificial Diels-Alderase. J. Am. Chem. Soc 2018, 140, 2862. [PubMed: 29406705] (h)Murase T; Nishijima Y; Fujita M Cage-Catalyzed Knoevenagel Condensation under Neutral Conditions in Water. J. Am. Chem. Soc 2012, 134, 162. [PubMed: 22145970] (i)Paul I; Goswami A; Mittal N; Schmittel M Catalytic Three-Component Machinery: Control of Catalytic Activity by Machine Speed. Angew. Chem.,

Int. Ed 2018, 57, 354.(j)Roy B; Devaraj A; Saha R; Jharimune S; Chi K-W; Mukherjee PS Catalytic Intramolecular Cycloaddition Reactions by Using a Discrete Molecular Architecture. Chem. - Eur. J 2017, 23, 15704. [PubMed: 28815866]

(12) (a). Hua Y; Flood AH Flipping the Switch on Chloride Concentrations with a Light-Active Foldamer. J. Am. Chem. Soc 2010, 132, 12838. [PubMed: 20799723] (b)Wei S-C; Pan M; Fan Y-Z; Liu H; Zhang J; Su C-Y Creating Coordination-Based Cavities in a Multiresponsive Supramolecular Gel. Chem. - Eur. J 2015, 21, 7418. [PubMed: 25876958]

(13) (a). Dhers S; Mondal A; Aguilà D; Ramirez J; Vela S; Dechambenoit P; Rouzieres M; Nitschke JR; Clérac R; Lehn J-M Spin State Chemistry: Modulation of Ligand pKa by Spin State Switching in a [2× 2] Iron (II) Grid-Type Complex. J. Am. Chem. Soc 2018, 140, 8218. [PubMed: 29874065] (b)Han M; Luo Y; Damaschke B; Gómez L; Ribas X; Jose A; Peretzki P; Seibt M; Clever GH Light-Controlled Interconversion between a Self-Assembled Triangle and a Rhombicuboctahedral Sphere. Angew. Chem., Int. Ed 2016, 55, 445.(c)Han M; Michel R; He B; Chen YS; Stalke D; John M; Clever GH Light-Triggered Guest Uptake and Release by a Photochromic Coordination Cage. Angew. Chem., Int. Ed 2013, 52, 1319.(d)Jansze SM; Cecot G; Severin K Reversible disassembly of metallasupramolecular structures mediated by a metastable-state photoacid. Chem. Sci 2018, 9, 4253. [PubMed: 29780555] (e)Piotrowski H; Severin K A self-assembled, redox-responsive receptor for the selective extraction of LiCl from water. Proc. Natl. Acad. Sci. U. S. A 2002, 99, 4997. [PubMed: 11959951] (f)Yan X; Xu J-F; Cook TR; Huang F; Yang Q-Z; Tung C-H; Stang PJ Photoinduced transformations of stiff-stilbene-based discrete metallacycles to metallosupramolecular polymers. Proc. Natl. Acad. Sci. U. S. A 2014, 111, 8717. [PubMed: 24889610] (g)Zhang D; Nie Y; Saha ML; He Z; Jiang L; Zhou Z; Stang PJ Photoreversible [2] Catenane via the Host-Guest Interactions between a Palladium Metallacycle and β-Cyclodextrin. Inorg. Chem 2015, 54, 11807. [PubMed: 26637012]

(14) (a). Becker RS; Michl J Photochromism of Synthetic and Naturally Occurring 2H-Chromenes and 2H-Pyrans. J. Am. Chem. Soc 1966, 88, 5931.(b)Helmy S; Leibfarth FA; Oh S; Poelma JE; Hawker CJ; Read de Alaniz J Photoswitching Using Visible Light: A New Class of Organic Photochromic Molecules. J. Am. Chem. Soc 2014, 136, 8169. [PubMed: 24848124]

(15) (a). Guo X; Zhang D; Zhu D Logic Control of the Fluorescence of a New Dyad, Spiropyran-Perylene Diimide-Spiropyran, with Light, Ferric Ion, and Proton: Construction of a New Three-Input “AND” Logic Gate. Adv. Mater 2004, 16, 125.(b)Raymo FM; Alvarado RJ; Giordani S; Cejas MA Memory Effects Based on Intermolecular Photoinduced Proton Transfer. J. Am. Chem. Soc 2003, 125, 2361. [PubMed: 12590566] (c)Zhu L; Zhu M-Q; Hurst JK; Li ADQ Light-Controlled Molecular Switches Modulate Nanocrystal Fluorescence. J. Am. Chem. Soc 2005, 127, 8968. [PubMed: 15969571] (d)Giordani S; Raymo FM A Switch in a Cage with a Memory. Org. Lett 2003, 5, 3559. [PubMed: 14507172]

(16) (a). Setaro A; Bluemmel P; Maity C; Hecht S; Reich S Non-Covalent Functionalization of Individual Nanotubes with Spiropyran-Based Molecular Switches. Adv. Funct. Mater 2012, 22, 2425.(b)Zhang M; Hou X; Wang J; Tian Y; Fan X; Zhai J; Jiang L Light and pH Cooperative Nanofluidic Diode Using a Spiropyran-Functionalized Single Nanochannel. Adv. Mater 2012, 24, 2424. [PubMed: 22488964] (c)Yao W; Wang H; Cui G; Li Z; Zhu A; Zhang S; Wang J Tuning the Hydrophilicity and Hydrophobicity of the Respective Cation and Anion: Reversible Phase Transfer of Ionic Liquids. Angew. Chem 2016, 128, 8066.(d)Silvi S; Arduini A; Pochini A; Secchi A; Tomasulo M; Raymo FM; Baroncini M; Credi A A Simple Molecular Machine Operated by Photoinduced Proton Transfer. J. Am. Chem. Soc 2007, 129, 13378. [PubMed: 17935334] (e)Yildiz I; Impellizzeri S; Deniz E; McCaughan B; Callan JF; Raymo FM Supramolecular Strategies To Construct Biocompatible and Photoswitchable Fluorescent Assemblies. J. Am. Chem. Soc 2011, 133, 871. [PubMed: 21182323] (f)Byrne R; Diamond D Chemo/bio-sensor networks. Nat. Mater 2006, 5, 421. [PubMed: 16738672]

(17) (a). Shao N; Zhang Y; Cheung S; Yang R; Chan W; Mo T; Li K; Liu F Copper Ion-Selective Fluorescent Sensor Based on the Inner Filter Effect Using a Spiropyran Derivative. Anal. Chem 2005, 77, 7294. [PubMed: 16285678] (b)Li Y; Duan Y; Li J; Zheng J; Yu H; Yang R Simultaneous Nucleophilic-Substituted and Electrostatic Interactions for Thermal Switching of Spiropyran: A New Approach for Rapid and Selective Colorimetric Detection of Thiol-Containing Amino Acids. Anal. Chem 2012, 84, 4732. [PubMed: 22545785] (c)Champagne B;

Plaquet A; Pozzo J-L; Rodriguez V; Castet F Nonlinear Optical Molecular Switches as Selective Cation Sensors. J. Am. Chem. Soc 2012, 134, 8101. [PubMed: 22548499]

(18). Dryza V; Bieske EJ Electron injection and energy-transfer properties of spiropyran-cyclodextrin complexes coated onto metal oxide nanoparticles: toward photochromic light harvesting. J. Phys. Chem. C 2015, 119, 14076.

(19) (a). Chen L; Wu J; Schmuck C; Tian H A switchable peptide sensor for real-time lysosomal tracking. Chem. Commun 2014, 50, 6443.(b)Zhu L; Wu W; Zhu M-Q; Han JJ; Hurst JK; Li ADQ Reversibly Photoswitchable Dual-Color Fluorescent Nanoparticles as New Tools for Live-Cell Imaging. J. Am. Chem. Soc 2007, 129, 3524. [PubMed: 17335209] (c)Shao N; Jin J; Wang H; Zheng J; Yang R; Chan W; Abliz Z Design of Bis-spiropyran Ligands as Dipolar Molecule Receptors and Application to in Vivo Glutathione Fluorescent Probes. J. Am. Chem. Soc 2010, 132, 725. [PubMed: 20030359]

(20). Berkovic G; Krongauz V; Weiss V Spiropyrans and Spirooxazines for Memories and Switches. Chem. Rev 2000, 100, 1741. [PubMed: 11777418]

(21). Williams DE; Martin CR; Dolgopolova EA; Swifton A; Godfrey DC; Ejegbavwo OA; Pellechia PJ; Smith MD; Shustova NB Flipping the Switch: Fast Photoisomerization in a Confined Environment. J. Am. Chem. Soc 2018, 140, 7611. [PubMed: 29807417]

(22). Wagner K; Zanoni M; Elliott ABS; Wagner P; Byrne R; Florea LE; Diamond D; Gordon KC; Wallace GG; Officer DL A merocyanine-based conductive polymer. J. Mater. Chem. C 2013, 1, 3913.

(23). Bhat IA; Devaraj A; Zangrando E; Mukherjee PS A Discrete Self-Assembled Pd12 Triangular Orthobicupola Cage and its Use for Intramolecular Cycloaddition. Chem. - Eur. J 2018, 24, 13938. [PubMed: 29920829]

(24). Bhattacharyya S; Chowdhury A; Saha R; Mukherjee PS Multifunctional Self-Assembled Macrocycles with Enhanced Emission and Reversible Photochromic Behavior. Inorg. Chem 2019, 58, 3968. [PubMed: 30810042]

(25). Li Y; Tam AY-Y; Wong KM-C; Li W; Wu L; Yam VW-W Synthesis, Characterization, and the Photochromic, Luminescence, Metallogelation and Liquid-Crystalline Properties of Multifunctional Platinum(II) Bipyridine Complexes. Chem. - Eur. J 2011, 17, 8048. [PubMed: 21695737]

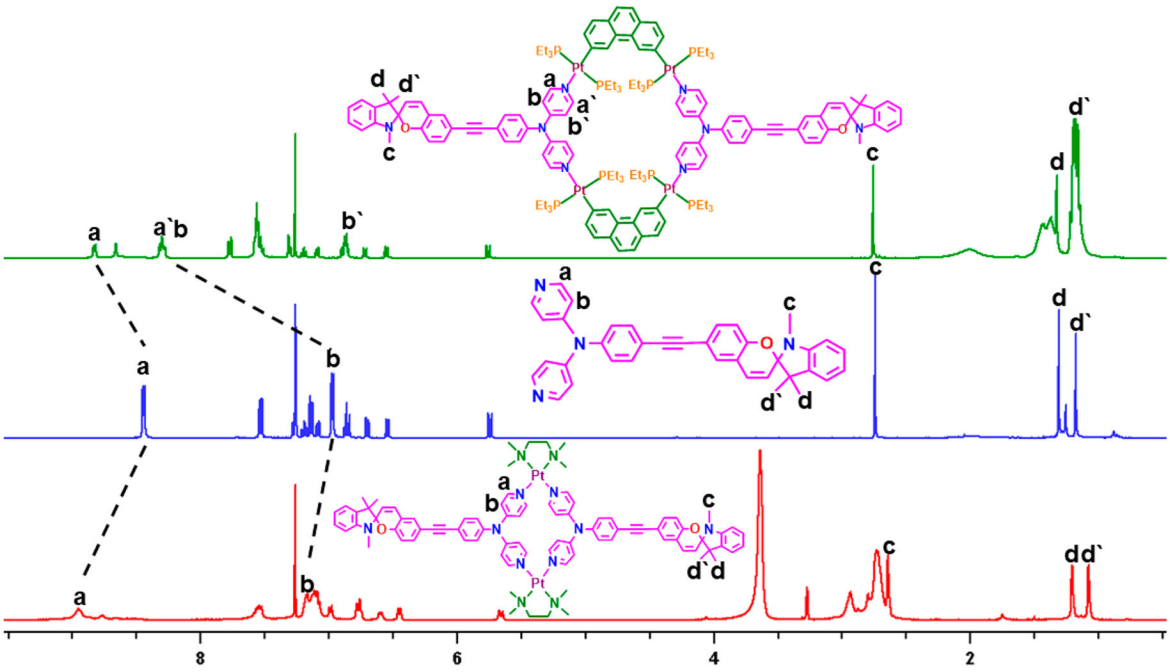

Figure 1.

Stacked ^{1}H NMR spectra of **6** (top), donor **2** (middle) in $CDCl_3$, and 7 (bottom) in $CDCl_3$ + CD_3OD (1:1).

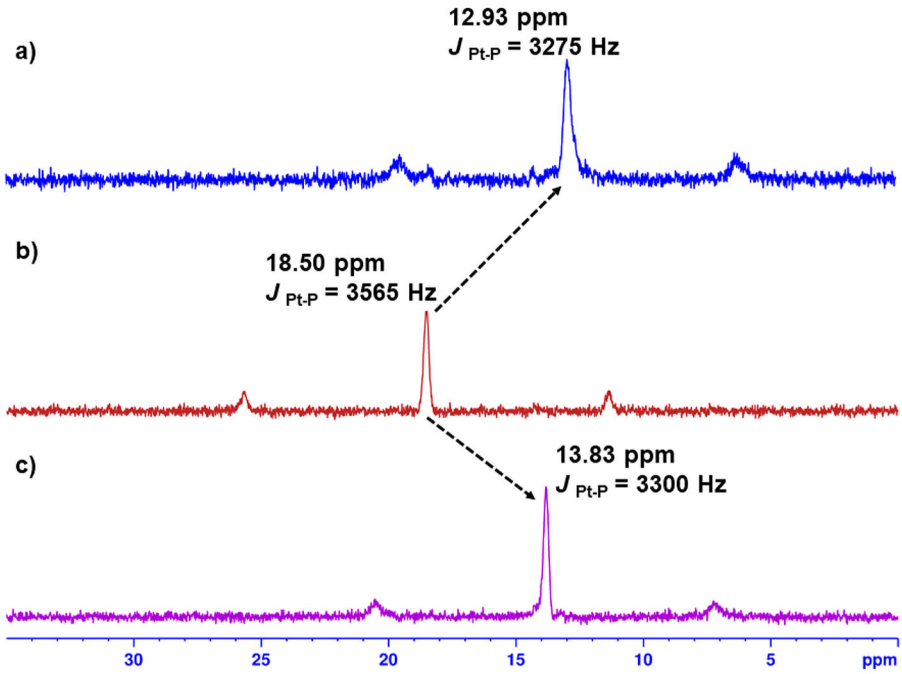

Figure 2.
^{31}P NMR spectra of acceptor **3** (b), **6** (c) in $CDCl_3$, and **5** (a) in CD_2Cl_2.

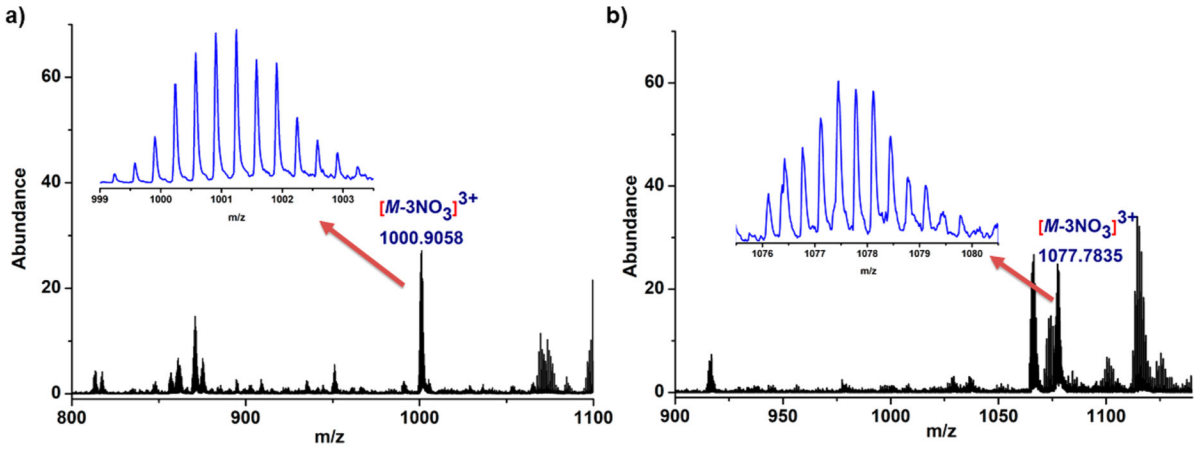

Figure 3.

Partial ESI-MS spectra of **5** (a) and **6** (b). Experimental isotopic patterns of their corresponding $[M - 3NO_3]^{3+}$ charge fragments (inset).

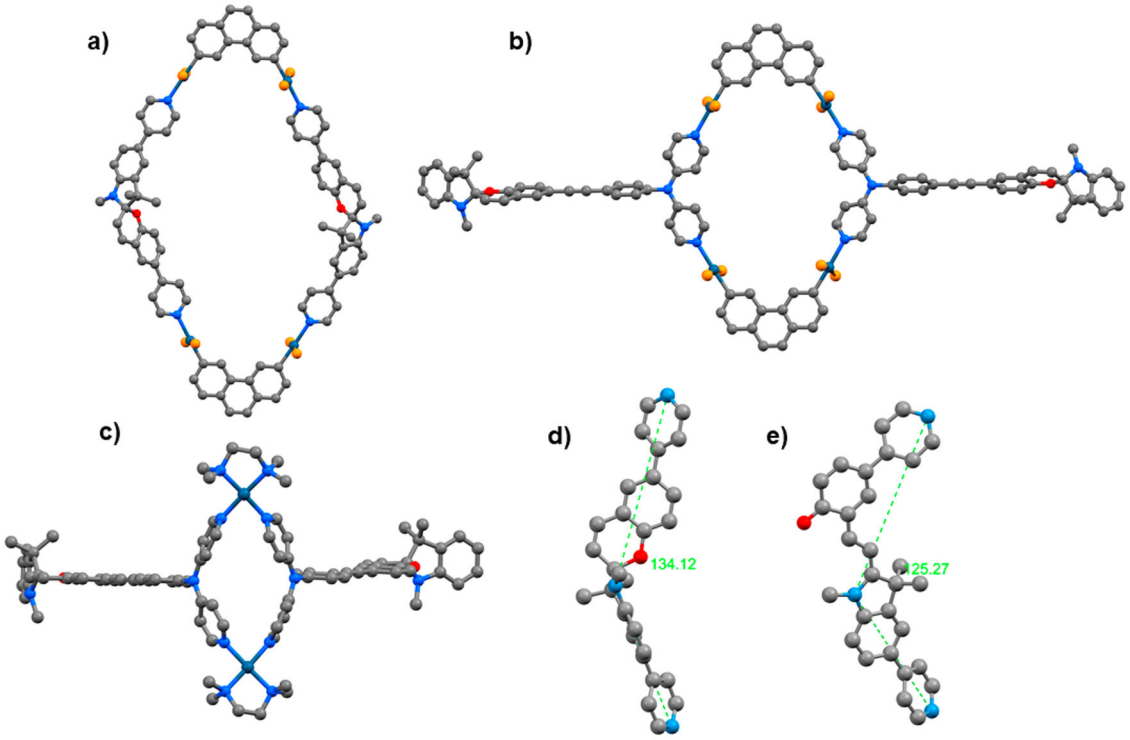

Figure 4.

Optimized structures of the macrocycles **5** (a), **6** (b), and 7 (c) and ring-closed (d) and ring-opened (e) isomers of donor **1**. Color code: C, gray; N, blue; O, red; P, orange; Pt, dark blue. H atoms omitted for clarity.

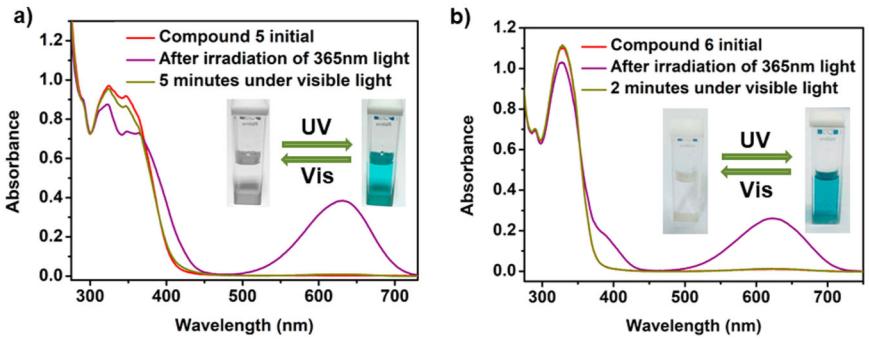

Figure 5.

Reversible photochromic behavior of **5** (a) and **6** (b) in DMSO. λ_{ex} = 365 nm and visible light.

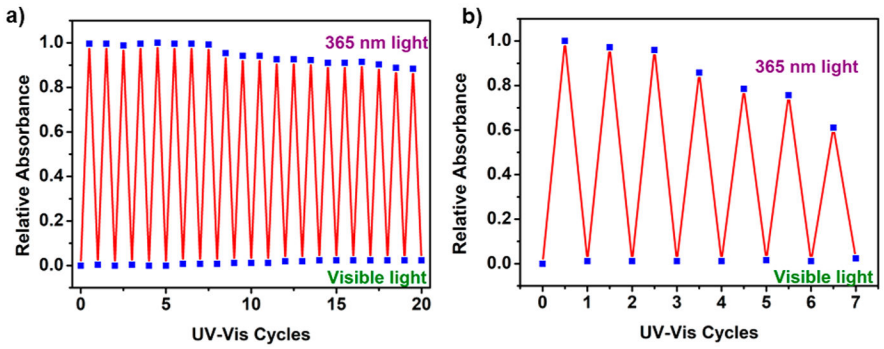

Figure 6.

Reversible photochromic cycles of **6** (a) and **5** (b) under UV- (365 nm) and visible-light exposure.

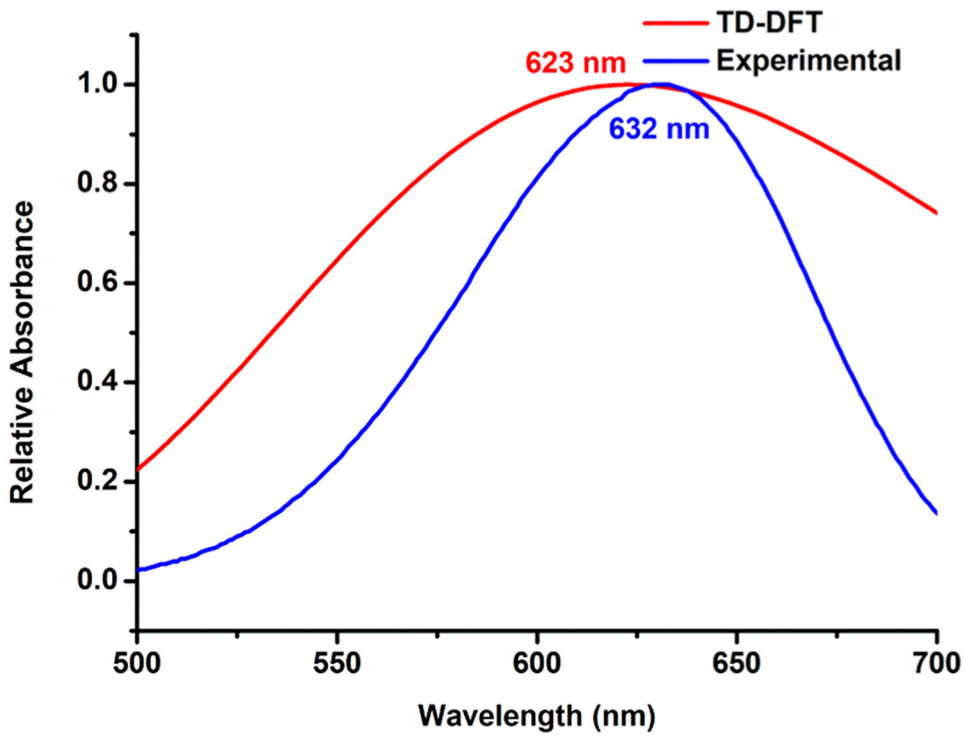

Figure 7.
Comparison of the experimental and theoretical (TD-DFT) UV–vis spectra for the photochromic behavior of **5**.

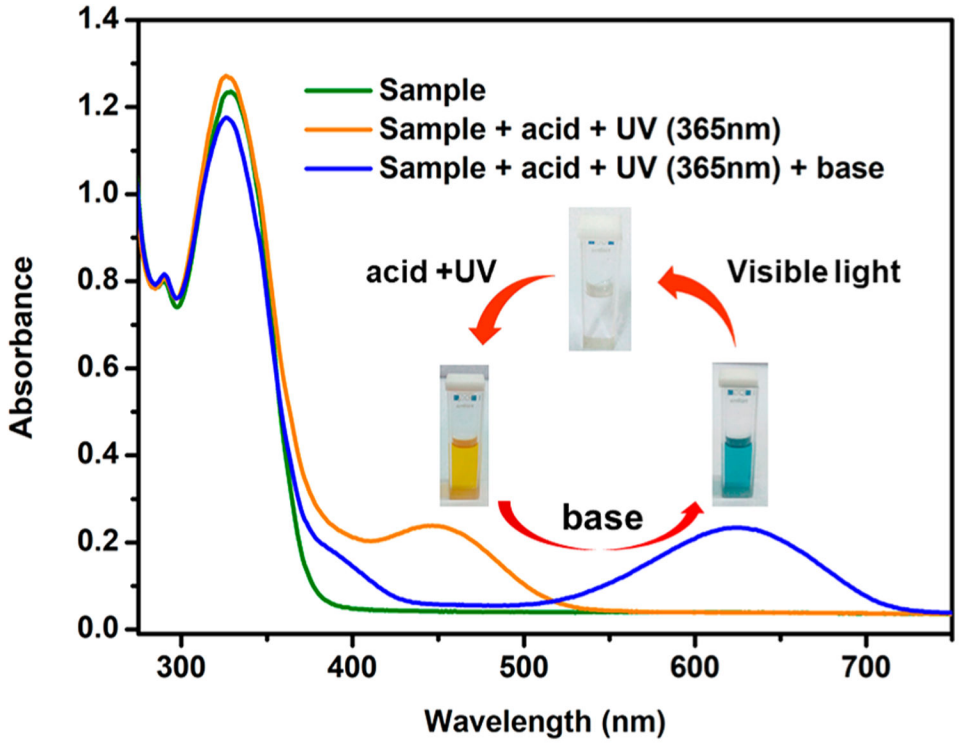

Figure 8.
Acidochromic behavior of the solution of **6** and its reversibility.

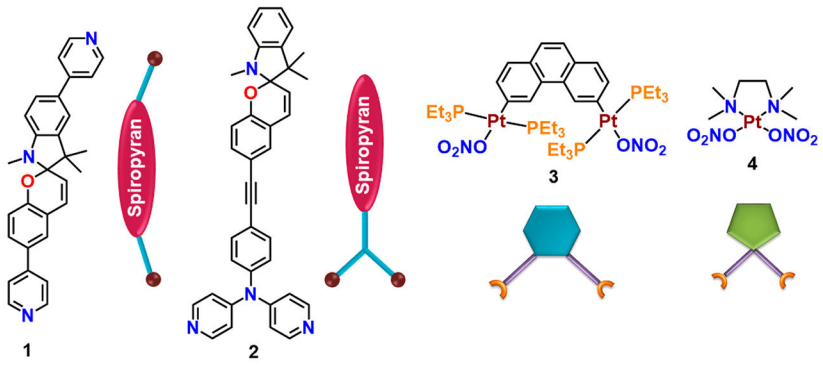

Scheme 1.

Structures of the Building Blocks 1–4 Used in the Synthesis of the Macrocycles

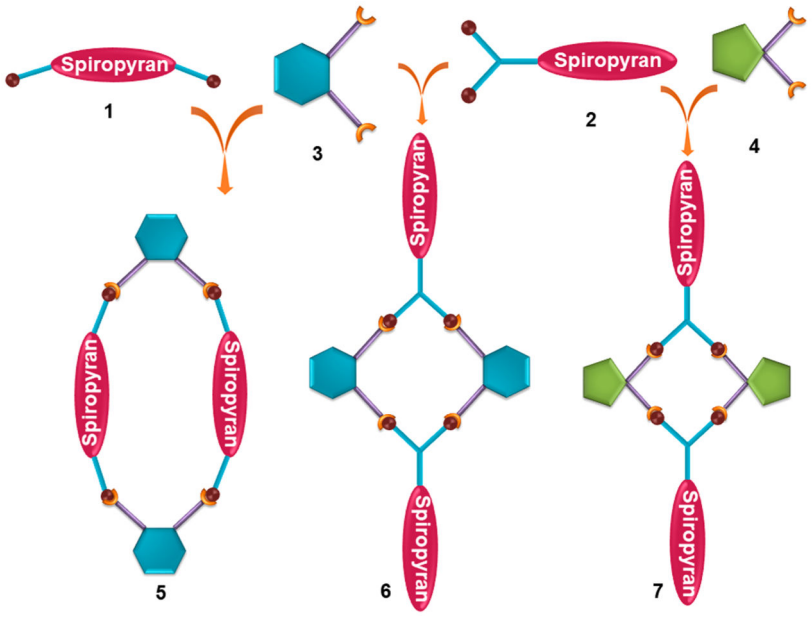

Scheme 2.

Self-Assembly of the Macrocycles 5–7 from Their Corresponding Building Blocks 1–4

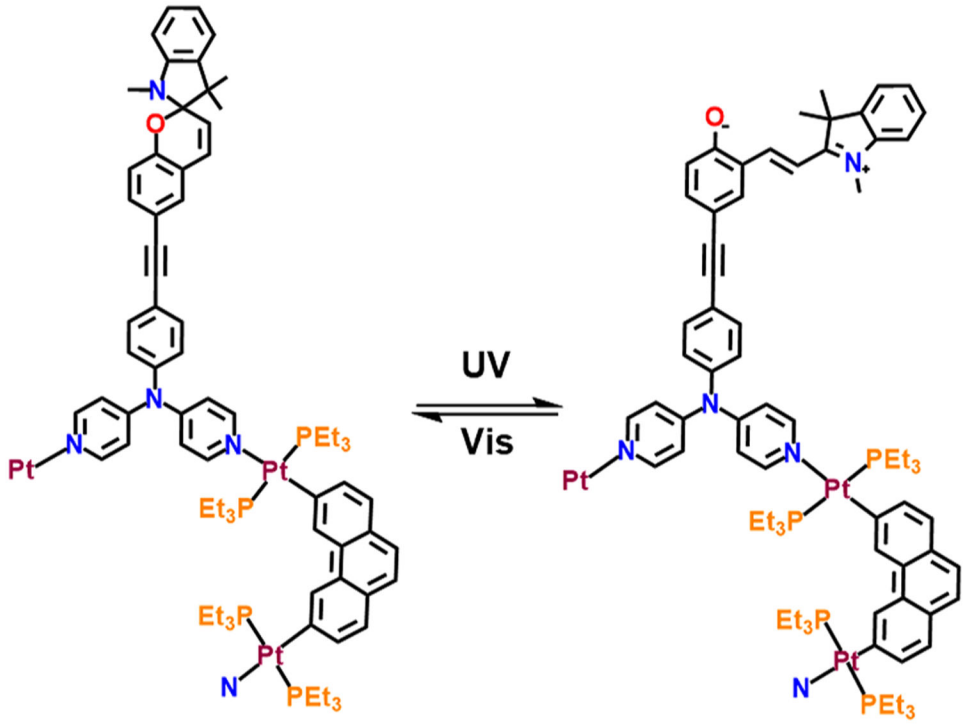

Scheme 3.
Partial Schematic Representation of the Photochromism of Macrocycle 6